




# Investigating the water vapor sorption behavior of bamboo with two sorption models

Xuexia Zhang<sup>1,2</sup>, Jing Li<sup>1,2</sup>, Yan Yu<sup>1,2</sup>, and Hankun Wang<sup>1,2,\*</sup> 

<sup>1</sup>Department of Biomaterials, International Center for Bamboo and Rattan, No. 8, Futong East Street, Wangjing Area, Chaoyang District, Beijing, People's Republic of China

<sup>2</sup>SFA and Beijing Co-built Key Lab for Bamboo and Rattan Science and Technology, Beijing, People's Republic of China

**Received:** 12 January 2018

**Accepted:** 22 February 2018

**Published online:**  
8 March 2018

© Springer Science+Business Media, LLC, part of Springer Nature 2018

## ABSTRACT

Studying the hygroscopic behavior of bamboo is important for industrial applications because it influences the dimensional stability and mechanical properties of the final bamboo products. In this study, the water vapor sorption behavior of 14 bamboo species was investigated using a dynamic vapor sorption apparatus and the results were analyzed using the Guggenheim–Anderson–de Boer (GAB) and Hailwood–Horrobin (H–H) models. The different bamboo species exhibited varying sorption isotherms and degrees of hysteresis. The reasons for this may be related to the different sorption isotherms of the two main cell units of bamboo, namely the fiber and parenchyma cells, and the chemical composition of bamboo. The GAB and H–H models provided good fits to the experimental data and meaningful physical parameters regarding the monolayer capacity, especially the water accessible specific surface area can be obtained from the GAB parameters. The fiber saturation point values were also determined using the GAB and H–H models, which ranged from 16.37 to 27.91% for the different bamboo species.

## Introduction

Bamboo is a grass that is abundant in tropical, subtropical and mild temperate regions and is one of the fastest growing plants on earth [1, 2]. Considering its rapid growth rate, low cost, high strength and stiffness, bamboo has been widely used in a variety of applications such as house construction, furniture, handicrafts and paper production, demonstrating its potential as a sustainable wood substitute [3, 4]. As a natural and heterogeneous material (like wood),

bamboo exhibits certain deleterious properties when subject to varying moisture levels, such as dimensional instability, mold growth, fungal decay and loss of strength [5, 6]. Consequently, it is important to understand the hygroscopic response of bamboo to its surrounding environment, in order to develop optimal drying processes and safe storage in varying conditions [7].

A sorption isotherm is often used to describe the relationship between the equilibrium moisture states of bamboo and its surrounding environment at

Address correspondence to E-mail: wanghankun@icbr.ac.cn

constant temperature and relative humidity (RH), and this includes the adsorption isotherm measured from an initial dry condition and the desorption one measured from an initially water-saturated condition [8, 9]. Although the water vapor sorption behavior of wood or chemically modified wood has been well documented, the investigations on bamboo were very limited [10, 11]. Therefore, there is a need to build knowledge on bamboo's water vapor sorption behavior to support and improve the processing and manufacturing of bamboo products.

The purpose of this study is to establish a statistically significant water vapor sorption database of bamboo species, as there are few studies in the literature that contains data for a wide range of bamboo species in one given study. Such information would be particularly useful in predicting the properties of bamboo in service and for modeling and optimizing the drying process. In this study, a dynamic vapor sorption (DVS) apparatus was used instead of saturated salt solutions as the former is more capable of providing highly reproducible data over a wide RH range [12].

## Materials and methods

### Sample preparations

Fourteen two-to-three-year bamboo species (Table 1) were obtained from the Hua'an arboretum in Fujian Province, China, for this study. All bamboo culms were selected randomly. Small bamboo blocks were

cut from the middle portion of the culm with a dimensions of  $10 \times 20 \times T$  mm (tangential  $\times$  longitudinal  $\times$  culm wall thickness) (Fig. 1a), and their waxy epidermises and pith rings were remained in order to gain the comprehensive hygroscopic behavior of raw bamboo samples. To limit bamboo variability caused by the hierarchical architecture with vascular bundles non-uniformly distributed along the radial direction (taking *M* species as an example, see Fig. 1a), small bamboo block (around 10 mg) containing the whole radial structure was cut from bamboo block of the same type, with a final dimensions of  $3 \times 1 \times T$  mm (tangential  $\times$  longitudinal  $\times$  culm wall thickness, Fig. 1b).

### Dynamic water vapor sorption

The water vapor sorption behavior of the bamboo samples was determined using a dynamic vapor sorption apparatus (DVS Intrinsic, Surface Measurement Systems Ltd., UK). The samples were placed on a holder connected to a microbalance ( $\pm 0.1 \mu\text{g}$ ) using hanging wires, and this was located in a thermostatically controlled chamber where a constant flow of dry nitrogen gas into which another flow of nitrogen containing a preset amount of water vapor was mixed to maintain a given RH [5]. The measurements were taken at a constant temperature of  $25 \pm 0.1$  °C for approximately 3 days, starting at 0% RH and increasing in increments of 10% RH up to 98% RH, then decreasing back to 0% RH also in 10% RH decrements. Samples were then maintained at a constant RH, until the weight change was less than

**Table 1** List of bamboo samples

Latin name	Age (year)	Notations
<i>Phyllostachys edulis</i> (Carr.) H. De Lehaie	3	M
<i>Phyllostachys heteroclada</i> Oliver	3	S
<i>Bambusa longispiculata</i> Gamble	3	HM
<i>Bambusa sinospinosa</i> McClure	3	CT
<i>Bambusa chungii</i> McClure	3	FD
<i>Bambusa rigida</i> Keng et Keng f.	3	YT
<i>Bambusa eutuldoides</i> McClure var. <i>viridi-vittata</i> (W. T. Lin) Chia	3	QS
<i>Bambusa emeiensis</i> L. C. Chia	3	C
<i>Bambusa multiplex</i> (Lour.) Raeuschel cv. Silverstripe R. A. Young	3	CL
<i>Dendrocalamus latiflorus</i> Munro	2	Ma
<i>Dendrocalamus giganteus</i> Munro	3	L
<i>Dendrocalamopsis vario-striata</i> (W. T. Lin) Keng f.	3	DS
<i>Dendrocalamopsis oldhami</i> (Munro) Keng f.	2	LV
<i>Sinocalmus affinis</i> (Rendle) McClure	3	LS

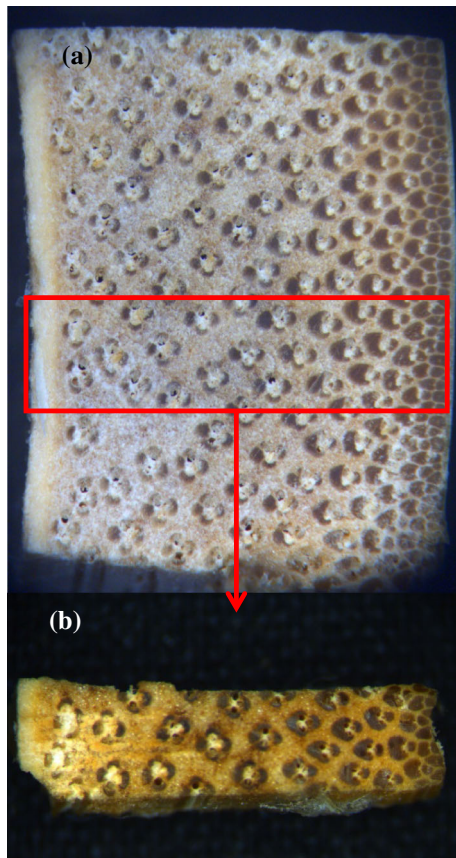


**Figure 1** Bamboo samples (*M* species as an example) used in the experiment.

0.002% per 10 min. Data on weight change were acquired every 20 s. As the DVS technique has been reported to yield highly reproducible data [13], in this study only one measurement is reported for each bamboo species.

### Sorption models

Several mathematical models have been developed to describe the water vapor sorption isotherms of hygroscopic materials [14]. The experimental sorption data of 14 bamboo species were fitted with two multilayer sorption models most frequently used for hygroscopic materials, namely the GAB and H–H models (Table 2). The GAB and H–H models represent two different theoretical concepts: the multilayer formation and water–polymer ideal solution assumption [11, 15]. The Origin 8.0 software (OriginLab Corporation, Northampton, MA, USA) was used for obtaining the parameters of the models. In addition, the fiber saturation point (FSP) values of

the 14 bamboo species were calculated using the two isotherm models.

### SEM observation

Sections of samples along the transverse and longitudinal directions were cut with blades and mounted on a sample holder with carbon conductive tape and then coated with a thin layer of platinum using a sputter coater (Leica EMSCD050). The morphology of samples was observed under a Field Emission Scanning Electron Microscope (FE-SEM, XL30, FEI, USA) operating at 7.0 kV.

## Results and discussion

### Adsorption and desorption isotherms

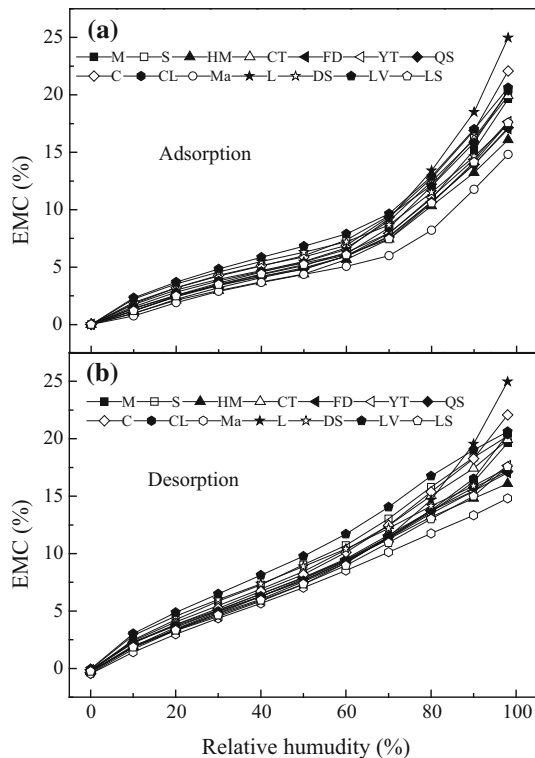
The water vapor adsorption and desorption isotherms of the 14 bamboo species are reported as the EMC against RH, presented in Fig. 2. All of the isotherms exhibited a sigmoidal shape typical of bamboo [10] and can be classified as type II according to the classification scheme of Brunauer et al. [16]. The adsorption isotherms of all bamboo species exhibited an upward bend at around 60–70% RH, whereas desorption isotherms were more linear at similar RH levels. Similar results were also reported in other studies on lignocellulosic materials [17, 18]. However, there were differences in the EMC values of the various bamboo species at certain RH levels, especially above 75% RH. At the highest RH (98%), *Ma* species reached an EMC of 14.81%, whereas the EMC of *L* species (belong to the same genus as *Ma* species) reached as high as 24.98%.

In addition to the difference in EMC values, there were also differences in the degree of hysteresis. Absolute hysteresis (obtained by subtracting the EMC of adsorption from the EMC of desorption isotherm at constant RH) and the hysteresis coefficient (a ratio of the EMC for adsorption to EMC for desorption at constant RH) are two common means to characterize sorption hysteresis [11, 13]. The changes in the absolute hysteresis and hysteresis coefficient are shown in Fig. 3. As shown in Fig. 3a, all bamboo species exhibited the hysteresis phenomenon over the entire RH region, but the degree of hysteresis varied. Hysteresis for all bamboo species increased first and then decreased with increasing

**Table 2** Sorption isotherm models for fitting experimental data

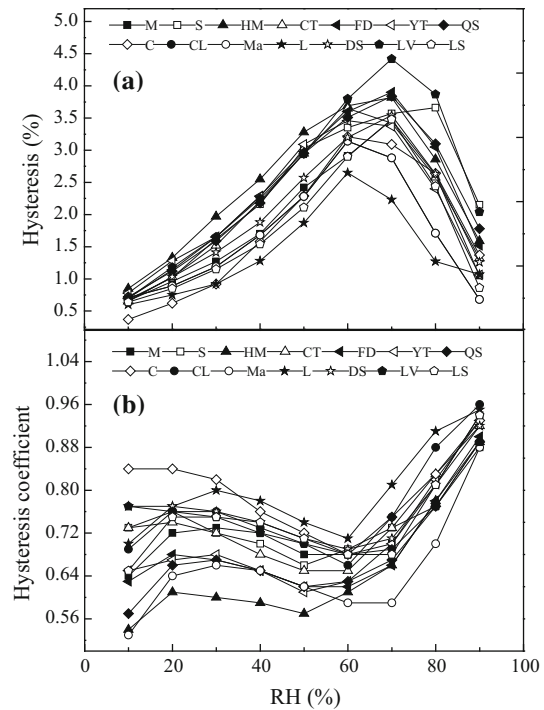
Models names	Models equations
GAB model	$EMC = \frac{100 \cdot X_m \cdot C \cdot K \cdot RH}{(100 - K \cdot RH) \cdot (100 + (C - 1) \cdot K \cdot RH)}$
H-H model	$EMC = M_h + M_s = \frac{1800}{W} \cdot \frac{K_1 \cdot K_2 \cdot RH}{100 + K_1 \cdot K_2 \cdot RH} + \frac{1800}{W} \cdot \frac{K_2 \cdot RH}{100 - K_2 \cdot RH}$

EMC, EMC of bamboo (%); RH, relative humidity (%);  $X_m$ , monolayer value (%);  $M_h$ , monolayer moisture content (%);  $M_s$ , multilayer moisture content (%);  $W$ , molecular weight of the cell wall polymer per adsorption site, and others are constants of the two models

**Figure 2** EMC values of 14 bamboo species plotted against RH during adsorption (a) and desorption (b).

RH, but the highest hysteresis values varied from 2.65 to 4.42% at 50–80% RH, depending on the species. The variation in the change in the hysteresis coefficient was remarkable (range 0.53–0.96) for the different bamboo species (Fig. 3b).

The water sorption and extent of hysteresis may be influenced by the structure and chemical composition of bamboo. On the one hand, the fine structure of different cell walls types plays a role in the hygroscopic behavior of bamboo [10]. Bamboo can be considered as a 2-phase composites consisting of fibers that are almost completely solid with insignificant lumen (Fig. 4c) embedded in parenchyma cells that are thin-walled and have large lumens (Fig. 4d) [19]. Adsorption/desorption isotherms and the

**Figure 3** Hysteresis (a) and hysteresis coefficient (b) of 14 bamboo species.

hysteresis for the fiber and parenchyma cells of *M* species are shown in Fig. 5, where it can be clearly seen that the parenchyma cells exhibited higher EMC values but lower hysteresis capacity at higher RH, indicating a difference in hygroscopic capacity from bamboo fibers. The reason for this may be related to the vast differences in the geometry of the cell walls as shown in Fig. 4. Therefore, the water vapor adsorption behavior of bamboo rested on the properties of the fibers and parenchyma cells and on the distribution of fibers.

On the other hand, hygroscopic behavior has also shown to differ in the main components of the cell wall, as hemicelluloses provide the highest number of OH groups available for water sorption, followed by cellulose and lignin [20]. Differences in the

**Figure 4** SEM images of the transverse section (a) and longitudinal section of *M* species (b), and partial magnifications of the bamboo fiber (c) and parenchyma cells (d).

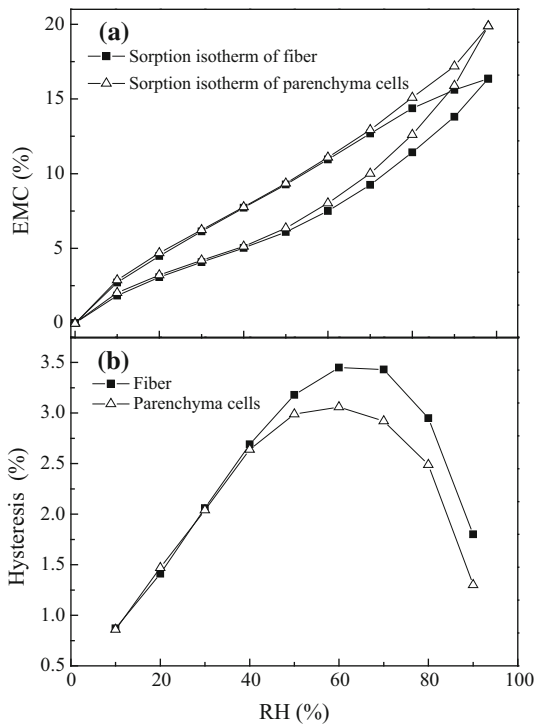
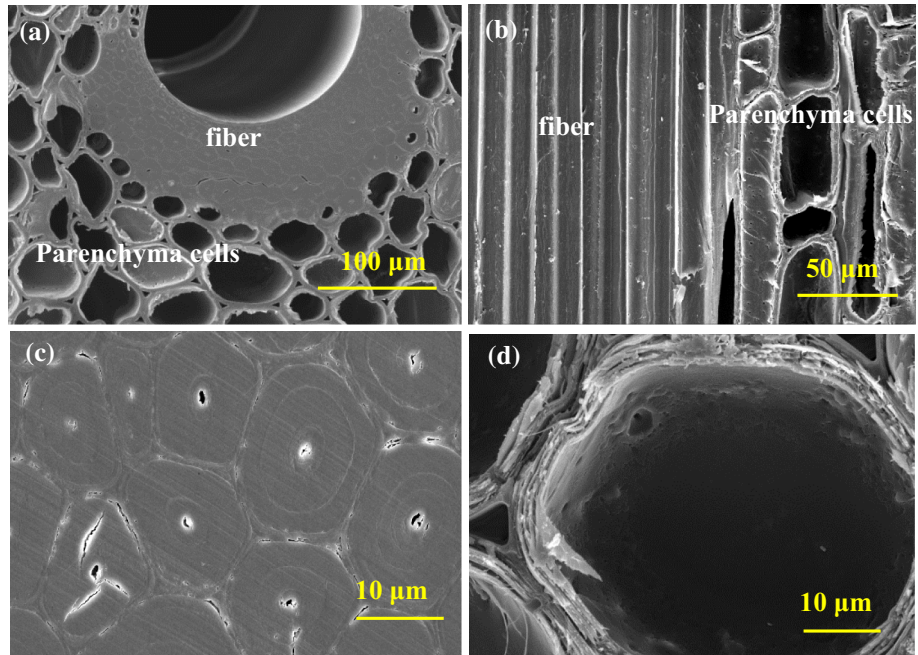


**Figure 5** Sorption isotherm (a) and hysteresis (b) of the fiber and parenchyma cells of *M* species.

contents of these components clearly have an effect on the water vapor sorption across bamboo species. Therefore, the variation in water sorption behavior of different bamboo species seems to be a very complex phenomenon and a more detailed study should be

conducted to explain the difference in the water sorption behavior of different bamboo species.

### Fitting the GAB model to the data

The results of fitting the GAB model to the data of the 14 bamboo species are presented in Table 3. The fits were considered to be valid as all the  $R^2$  values above 99.0% [21]. GAB parameters can be used to compare the hygroscopic properties of different bamboo species. Among them, the  $X_m$  (GAB) obtained from the adsorption branch refers to the moisture content when the monolayer is full and can be used to estimate the internal specific surface area corresponding to the monolayer capacity. The internal specific surface area ( $S_{GAB}$ ) is defined as

$$S_{GAB} = \frac{X_m \cdot \rho \cdot L \cdot \sigma}{M} \tag{1}$$

where  $\rho$  is water density,  $L$  is the Avogadro number,  $\sigma$  is the average area where water occupies the complete monolayer (0.114 nm<sup>2</sup> was used in this study), and  $M$  is the molar mass of water [22].

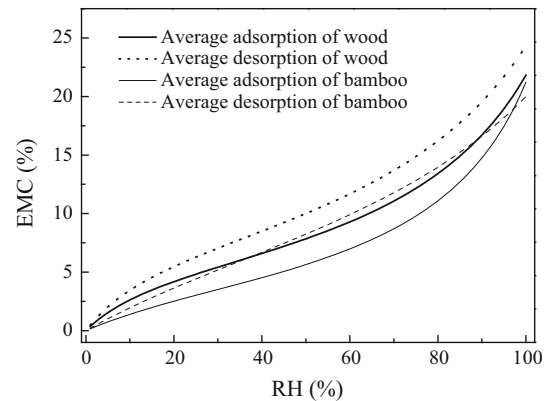
The obtained  $X_m$  value ranged from 3.26% for Ma species to 5.27% for HM species, and the corresponding  $S_{GAB}$  increased from 124 to 201 m<sup>2</sup>/g, which represented the lowest and the highest monolayer capacity. This is due to their differences in cell wall ultrastructure and chemical composition, as mentioned above. The  $C$  value in the GAB model is

**Table 3** Fitted model parameters and specific surface areas for 14 bamboo species obtained from the GAB model

Notations	Adsorption					Desorption			
	$X_m$ (%)	C	K	$R^2$ (%)	$S_{GAB}$ (m <sup>2</sup> /g)	$X_m$ (%)	C	K	$R^2$ (%)
M	4.26	4.15	0.81	99.716	162	7.78	3.84	0.66	99.917
S	4.86	5.71	0.79	99.778	185	11.01	3.76	0.57	99.757
HM	5.27	2.29	0.74	99.511	201	16.16	2.75	0.39	99.828
CT	4.98	4.23	0.79	99.289	190	9.54	4.03	0.61	99.866
FD	4.57	3.69	0.77	99.481	174	13.62	2.94	0.45	99.820
YT	4.62	3.65	0.78	99.302	176	8.70	4.45	0.59	99.907
QS	4.88	2.89	0.76	99.574	186	17.71	2.21	0.40	99.813
C	4.53	6.36	0.82	99.594	173	8.14	4.11	0.68	99.903
CL	4.42	4.69	0.81	99.326	169	6.65	5.48	0.71	99.930
Ma	3.26	4.96	0.81	99.418	124	14.68	2.61	0.39	99.875
L	5.14	2.72	0.83	99.556	196	6.25	4.10	0.78	99.945
DS	4.61	9.69	0.76	99.610	176	9.73	5.84	0.53	99.843
LV	5.01	8.29	0.79	99.609	191	12.09	4.38	0.53	99.665
LS	4.20	4.70	0.79	99.501	160	8.77	3.55	0.60	99.900
‘Average’ bamboo	4.47	4.70	0.80	95.688	170	9.07	3.91	0.61	96.166
Standard error	0.303	1.0144	0.013			1.041	0.668	0.0329	
‘Average’ wood [22]	5.9	8.8	0.74			7.9	9.24	0.69	

the total heat of sorption of the monolayer and is always positive due to the strong exothermic interaction between the water vapor and adsorption sites [21]. Also, the  $K$  value is a factor that corrects the properties of the multilayer molecules with respect to the bulk liquid, which is unsound when higher than one as sorption becomes infinite at water activity values lower than one [23]. Moreover, the value of  $K$  given in Table 3 of ca. 0.8 (range: 0.74–0.83) can be taken as the characteristic of a non-porous sorbent [24].

The hygroscopic difference between bamboo and wood species was further compared. Here, the average GAB constants with corresponding uncertainties were obtained by fitting the entire sets of adsorption data to all 14 bamboo species. The average GAB constants of 21 wood species were also obtained by Bratasz et al. [22]. The average GAB constants of bamboo and wood species are given in Table 3, and the two general isotherms are shown in Fig. 6. It can be clearly observed that bamboo generally exhibits less hygroscopicity than wood during the both adsorption and desorption process.

**Figure 6** Average adsorption and desorption isotherms of wood and bamboo obtained from the GAB model.

### Fitting data to the H–H model

The results of fitting experimental data to the H–H model are shown in Table 4. Like the GAB model, the H–H model also demonstrated satisfactory fitting to the experimental data ( $R^2 \geq 99\%$ ). The  $W$  value represents the apparent molecular mass of the dry bamboo per sorption, and  $K_1$  and  $K_2$  are equilibrium constants related to the formation of hydrates from dissolved water and the dry bamboo material, and the formation between dissolved water and external water vapor [18]. The value of  $W$  for Ma species

**Table 4** Fitted model parameters for 14 bamboo species obtained from the H–H model

Notations	Adsorption				Desorption			
	W	$K_1$	$K_2$	$R^2$ (%)	W	$K_1$	$K_2$	$R^2$ (%)
M	423.00	3.15	0.81	99.716	231.38	2.84	0.66	99.917
S	370.24	4.71	0.79	99.778	163.41	2.76	0.57	99.757
HM	341.52	1.29	0.74	99.511	111.37	1.75	0.39	99.828
CT	361.63	3.23	0.79	99.289	188.60	3.03	0.61	99.866
FD	394.14	2.69	0.77	99.481	132.18	1.94	0.45	99.820
YT	389.51	2.64	0.78	99.302	206.78	3.45	0.59	99.907
QS	368.88	1.88	0.76	99.574	101.62	1.21	0.40	99.813
C	397.29	5.35	0.82	99.594	221.12	3.11	0.68	99.903
CL	407.42	3.69	0.81	99.326	270.51	4.48	0.71	99.930
Ma	552.14	3.96	0.81	99.418	122.63	1.61	0.39	99.875
L	350.56	1.72	0.83	99.556	287.84	3.10	0.78	99.945
DS	390.11	8.69	0.76	99.610	184.95	4.84	0.53	99.843
LV	358.97	7.28	0.79	99.609	148.91	3.38	0.53	99.665
LS	428.57	3.70	0.79	99.501	205.31	2.55	0.60	99.900

(552.14) was remarkably higher than that of other species, indicating that it had less available sites than others, which agreed with the lower EMC of Ma species observed in Fig. 2a. The value of  $K_2$  ranged from 0.74 to 0.83 which indicates that the dissolved water had lower activity than the liquid water, which was close to the value of  $K_2$  (0.72) for wood [25] and a little higher than the value of  $K_2$  (0.619–0.682) for paper materials [18].

According to the H–H model, the sigmoidal isotherms can be divided into monolayer ( $M_h$ ) and multilayer ( $M_s$ ) water, referring, respectively, to hydrates and dissolved water. As an example, Fig. 7 demonstrates that the fit was generally satisfactory over the whole RH range for M species. The results showed that monolayer water increased at the low

RH region, indicating that the water that is directly bound to active sites is mainly with hydroxyl groups, and with increasing RH, water preferentially adsorbs already hydrogen-bonded molecules and forms clusters to form polylayer water.

### Comparison of models

Knowledge of the monolayer moisture content of lignocellulosic materials is important for industrial applications, as it corresponds to ensuring the stability of the material to minimize spoilage [26]. The comparison between the GAB and H–H models on determining monolayer moisture content is shown in Table 5. The results showed that the GAB model exhibited higher monolayer moisture content than the H–H model, and this is due to their difference in mathematical expression and physical concepts on monolayer sorption. Higher monolayer moisture contents obtained from GAB model than H–H model were also reported for paper samples [18].

FSP is defined as the moisture content corresponding to the saturation of the cell wall with no free water in the cell lumen [27]. Knowledge of the FSP values of lignocellulosic materials is necessary because it influences the dimensional changes and mechanical strength of materials [28]. The EMC obtained in adsorption isotherms at 100% RH is considered as the nominal FSP value. In contrast to the difference in monolayer moisture content, the nominal FSP value determined from the GAB and H–H models was the same given that their mathematical

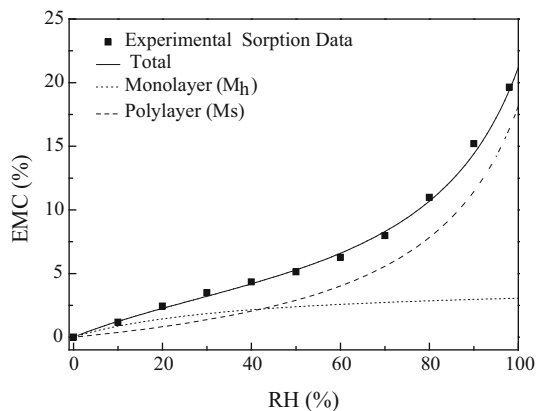


**Figure 7** Water vapor adsorption experimental data showing agreement with the H–H model (M species).

**Table 5** Comparison of monolayer moisture contents obtained from the H–H and GAB models

Notations	Monolayer moisture content ( $M_h$ , %)		Fiber saturation point (FSP, %)
	GAB model	H–H model	
M	4.26	3.06	21.74
S	4.86	3.83	22.14
HM	5.27	2.57	17.43
CT	4.98	3.57	21.91
FD	4.57	3.08	18.64
YT	4.62	3.11	19.40
QS	4.88	2.88	18.67
C	4.53	3.69	24.48
CL	4.42	3.31	22.62
Ma	3.26	2.49	16.36
L	5.14	3.02	27.91
DS	4.61	4.01	18.95
LV	5.01	4.27	22.59
LS	4.20	3.13	19.31

structures are similar [11]. As shown in Table 5, the FSP value varied from 16.36% for Ma species and 27.91% for L species, and the differences are mainly seen at high RH levels. However, it has been argued whether FSP value can be accurately extrapolated using sorption isotherms, because the adsorption isotherm increases sharply in the vicinity of 100% RH and large errors may arise from slight errors [29]. It is best to determine FSP value using other appropriate tests, such as volumetric swelling intersection [28] and pressure plate methods [30].

## Conclusions

In this study, the hygroscopic behavior of 14 bamboo species was determined from their water vapor sorption isotherms at 25 °C in the range of 0–98% RH. The different bamboo species exhibited variable water vapor sorption isotherm as the EMC values and the degree of hysteresis observed varied throughout all RH levels. All sorption isotherms exhibited typical type II isotherms and could be predicted agreeably with GAB and H–H models. The values of monolayer moisture content for 14 bamboo species as estimated by the GAB and H–H models ranged from 3.26 to 5.27%, 2.49 to 3.83%, respectively. In particular, the internal specific surface area of bamboo was calculated from the GAB monolayer parameter, varying from 124 to 201 m<sup>2</sup>/g. Moreover, the ‘average’ sorption isotherm of bamboo can be obtained from the sorption data, which exhibited less

hygroscopicity than wood. The information generated in this study can provide useful information in modeling the hygroscopic responses of bamboo in environments with changing moisture levels.

## Acknowledgements

We would like to thank the National Science Foundation of China (31400519) and 12th Five Years Key Technology R&D Program (2015BAD04B03) for their financial support for this research.

## Compliance with ethical standards

**Conflict of interest** The authors declared that they have no conflict of interest.

## References

- [1] Brito BSL, Pereira FV, Putaux JL, Jean B (2012) Preparation, morphology and structure of cellulose nanocrystals from bamboo fibers. *Cellulose* 19(5):1527–1536
- [2] Ohmae Y, Saito Y, Inoue M, Nakano T (2009) Mechanism of water adsorption capacity change of bamboo by heating. *Eur J Wood Wood Prod* 67(1):13–18
- [3] Ahmad M, Kamke FA (2005) Analysis of Calcutta bamboo for structural composite materials: physical and mechanical properties. *Wood Sci Technol* 39(6):448–459
- [4] Wang YY, Yin H (2014) Analysis on significance of bamboo products based on sustainable development. *Adv Mater Res* 1010–1012:1944–1948



- [5] Čermák P, Vahtikari K, Rautkari L, Laine K, Horáček P, Baar J (2016) The effect of wetting cycles on moisture behaviour of thermally modified Scots pine (*Pinus sylvestris* L.) wood. *J Mater Sci* 51(3):1–8. <https://doi.org/10.1007/s10853-015-9471-5>
- [6] Popescu CM, Hill CAS, Curling S, Ormondroyd G, Xie Y (2014) The water vapour sorption behaviour of acetylated birch wood: how acetylation affects the sorption isotherm and accessible hydroxyl content. *J Mater Sci* 49(5):2362–2371. <https://doi.org/10.1007/s10853-013-7937-x>
- [7] Rhim JW, Lee JH (2009) Thermodynamic analysis of water vapor sorption isotherms and mechanical properties of selected paper-based food packaging materials. *J Food Sci* 74(9):E502–E511
- [8] Zelinka SL, Mitchell MR, Link RE, Glass SV (2010) Water vapor sorption isotherms for southern pine treated with several waterborne preservatives. *J Test Eva* 38(4):521–525
- [9] Englund ET, Thygesen LG, Svensson S, Hill CAS (2013) A critical discussion of the physics of wood–water interactions. *Wood Sci Technol* 47(1):141–161
- [10] Ohmae Y, Nakano T (2009) Water adsorption properties of bamboo in the longitudinal direction. *Wood Sci Technol* 43(5–6):415–422
- [11] Olek W, Majka J, Czajkowski Ł (2013) Sorption isotherms of thermally modified wood. *Holzforschung* 67(2):183–191
- [12] Rautkari L, Hill CAS, Curling S, Jalaludin Z, Ormondroyd G (2013) What is the role of the accessibility of wood hydroxyl groups in controlling moisture content? *J Mater Sci* 48(18):6352–6356. <https://doi.org/10.1007/s10853-013-7434-2>
- [13] Xie Y, Hill CAS, Jalaludin Z, Curling SF, Anandjiwala RD, Norton AJ, Newman G (2011) The dynamic water vapour sorption behaviour of natural fibres and kinetic analysis using the parallel exponential kinetics model. *J Mater Sci* 46(2):479–489. <https://doi.org/10.1007/s10853-010-4935-0>
- [14] Simpson W (1980) Sorption theories applied to wood. *Wood Fiber* 12(3):183–195
- [15] Papadopoulos AN, Avramidis S, Elustondo D (2005) The sorption of water vapour by chemically modified softwood: analysis using various sorption models. *Wood Sci Technol* 39(2):99–111
- [16] Brunauer S, Deming LS, Deming WE, Teller E (1940) On a theory of the van der Waals adsorption of gases. *J Am Chem Soc* 62(7):1723–1732
- [17] Hill CAS, Norton A, Newman G (2009) The water vapor sorption behavior of natural fibers. *J Appl Polym S* 112(3):1524–1537
- [18] Bedane AH, Xiao H, Eić M (2014) Water vapor adsorption equilibria and mass transport in unmodified and modified cellulose fiber-based materials. *Adsorption* 20(7):863–874
- [19] Zhang X, Li J, Yu Z, Yu Y, Wang H (2017) Compressive failure mechanism and buckling analysis of the graded hierarchical bamboo structure. *J Mater Sci* 52(12):6999–7007. <https://doi.org/10.1007/s10853-017-0933-9>
- [20] Christensen GN, Kelsey KE (1959) The rate of sorption of water vapor by wood. *Holz als Roh- und Werkstoff* 17(5):178–188
- [21] Esteban LG, Simón C, Fernández FG, Palacios PD, Martín-Sampedro R, Eugenio ME, Hosseinpourpia R (2015) Juvenile and mature wood of *Abies pinsapo* Boissier: sorption and thermodynamic properties. *Wood Sci Technol* 49(4):725–738
- [22] Bratasz Ł, Kozłowska A, Kozłowski R (2012) Analysis of water adsorption by wood using the Guggenheim–Anderson–de Boer equation. *Eur J Wood Wood Prod* 70(4):445–451
- [23] Maskan M, Göğüş F (1997) The fitting of various models to water sorption isotherms of pistachio nut paste. *J Food Eng* 33(3–4):227–237
- [24] Timmermann EO (2003) Multilayer sorption parameters: BET or GAB values? *Colloids Surf A* 220(1–3):235–260
- [25] Mantanis GI, Papadopoulos AN (2010) The sorption of water vapour of wood treated with a nanotechnology compound. *Wood Sci Technol* 44(3):515–522
- [26] Moreira R, Chenlo F, Torres MD, Vallejo N (2008) Thermodynamic analysis of experimental sorption isotherms of loquat and quince fruits. *J Food Eng* 88(4):514–521
- [27] Tiemann H (1906) Effect of moisture upon the strength and stiffness of wood, vol 63. US Dept. of Agriculture, Forest Service, Washington, D.C.
- [28] Hernández R (2007) Effects of extraneous substances, wood density and interlocked grain on fiber saturation point of hardwoods. *Wood Mater Sci Eng* 2(1):45–53
- [29] Hill CAS (2008) The reduction in the fibre saturation point of wood due to chemical modification using anhydride reagents: a reappraisal. *Holzforschung* 62(4):423–428
- [30] Hernandez RE, Pontin M (2006) Shrinkage of three tropical hardwoods below and above the fiber saturation point. *Wood Fiber Sci* 38(3):474–483